PLOS ONE

RESEARCH ARTICLE

Addiction of mesenchymal phenotypes on the FGF/FGFR axis in oral squamous cell carcinoma cells

Asami Hotta Osada[1,2,3], Kaori Endo[1], Yujiro Kimura[1,2], Kei Sakamoto[4], Ryosuke Nakamura[3,5], Kaname Sakamoto[1], Koichiro Ueki[2], Kunio Yoshizawa[2], Keiji Miyazawa[1], Masao Saitoh[1,3]*

1 Department of Biochemistry, Interdisciplinary Graduate School of Medicine, University of Yamanashi, Chuo, Yamanashi, Japan, **2** Department of Oral and Maxillofacial Surgery, Interdisciplinary Graduate School of Medicine, University of Yamanashi, Chuo, Yamanashi, Japan, **3** Center for Medical Education and Sciences, Interdisciplinary Graduate School of Medicine, University of Yamanashi, Chuo, Yamanashi, Japan, **4** Department of Oral Pathology, Graduate School of Medical and Dental Sciences, Tokyo Medical and Dental University, Yushima, Bunkyo-ku, Tokyo, Japan, **5** Department of Oral Surgery, Kofu Municipal Hospital, Kofu, Yamanashi, Japan

* msaitoh-ind@umin.ac.jp

Citation: Osada AH, Endo K, Kimura Y, Sakamoto K, Nakamura R, Sakamoto K, et al. (2019) Addiction of mesenchymal phenotypes on the FGF/FGFR axis in oral squamous cell carcinoma cells. PLoS ONE 14(11): e0217451. https://doi.org/10.1371/journal.pone.0217451

Editor: Masaru Katoh, National Cancer Center, JAPAN

Received: May 9, 2019

Accepted: September 17, 2019

Published: November 4, 2019

Data Availability Statement: All relevant data are within the manuscript and its Supporting Information files.

Funding: This study was supported by the Mitsubishi Foundation, JSPS KAKENHI grant number 18H02969, and JSPS KAKENHI grant number 15H05018.

Competing interests: The authors have declared that no competing interests exist.

Abstract

The epithelial–mesenchymal transition (EMT) is a crucial morphological event that occurs during epithelial tumor progression. ZEB1/2 are EMT transcription factors that are positively correlated with EMT phenotypes and breast cancer aggressiveness. ZEB1/2 regulate the alternative splicing and hence isoform switching of fibroblast growth factor receptors (FGFRs) by repressing the epithelial splicing regulatory proteins, ESRP1 and ESRP2. Here, we show that the mesenchymal-like phenotypes of oral squamous cell carcinoma (OSCC) cells are dependent on autocrine FGF–FGFR signaling. Mesenchymal-like OSCC cells express low levels of ESRP1/2 and high levels of ZEB1/2, resulting in constitutive expression of the IIIc-isoform of FGFR, FGFR(IIIc). By contrast, epithelial-like OSCC cells showed opposite expression profiles for these proteins and constitutive expression of the IIIb-isoform of FGFR2, FGFR2(IIIb). Importantly, ERK1/2 was constitutively phosphorylated through FGFR1(IIIc), which was activated by factors secreted autonomously by mesenchymal-like OSCC cells and involved in sustained high-level expression of ZEB1. Antagonizing FGFR1 with either inhibitors or siRNAs considerably repressed ZEB1 expression and restored epithelial-like traits. Therefore, autocrine FGF–FGFR(IIIc) signaling appears to be responsible for sustaining ZEB1/2 at high levels and the EMT phenotype in OSCC cells.

Introduction

Oral tongue squamous cell carcinoma (OSCC) is one of the most common malignancies in head and neck cancers[1]. Most patients on their first visit to hospitals are diagnosed with locoregional initial symptoms of the disease. After various treatments, including surgical operation, chemotherapy, radiotherapy, or combination, the five-year survival rate remains less

Abbreviations: EMT, epithelial–mesenchymal transition; TGF-β, transforming growth factor-β; qPCR, quantitative real-time PCR; RT-qPCR, reverse transcription qPCR; siRNA, small interfering RNA; OSCC, oral squamous cell carcinoma; ESRP, epithelial splicing regulatory protein; FGF, fibroblast growth factor; FGFR, fibroblast growth factor receptor.

than 50% due to its aggressive invasiveness and resistance to treatments[2]. Thus, the development of diagnostic and therapeutic strategy would be of significant benefit to the development of successful therapies.

The process of cancer cell invasion involves the loss of cell–cell interactions along with the acquisition of motility, and is partly associated with the epithelial–mesenchymal transition (EMT)[3]. EMT involves dramatic cellular changes in which epithelial cells loosen their attachments to neighboring cells, lose their apico-basal polarity, become elongated, and display increased motility. EMT therefore forms the first step of the invasion–metastasis cascade. After invading through basement membranes and blood/lymphatic vessel walls, cells undergoing EMT survive in the bloodstream as circulating tumor cells, and, lastly, extravasate into distant organs. Upon arriving at distant metastasized tissues, the cancer cells undergo a reversion process, the mesenchymal–epithelial transition (MET)[4, 5]. The EMT process is regulated by several transcription factors known as EMT transcription factors (EMT-TFs), including the δEF1 family of two-handed zinc-finger factors (ZEB1 [Zinc-finger E-box binding homeobox 1]/δEF1 [δ-crystallin/E2-box factor 1] and ZEB2/SIP1 [Smad-interacting protein1]), the Snai1 family (Snail, Slug, and Smuc), and basic helix-loop-helix factors (Twist and E12/E47). Among these, the levels of ZEB1/2 in particular correlate positively with EMT phenotypes and the aggressiveness of breast cancer cells[6, 7]. It remains unclear, however, why expression of ZEB1/2 is sustained at high levels in aggressive cancer cells.

The alternative splicing machinery is also involved in regulating EMT[4]. Epithelial splicing regulatory proteins (ESRPs) 1 and 2, also known as RNA-recognition motif–containing proteins Rbm35a and Rbm35b, respectively, induce the switching of alternative splicing of transcripts, such as fibroblast growth factor receptors (FGFRs), CD44, Rac1, p120 catenin, and Mena. ZEB1/2 are preferentially recruited to the promoter region of *ESRP1*, and suppress the transcription of *ESRP1* during EMT[8, 9]. Despite the similar primary structures of the ESRP1 and ESRP2 proteins, the functions of the two proteins differ slightly in OSCC cells[10].

The *FGFR* genes encode four functional receptors (FGFR1–4) with three extracellular immunoglobulin-like domains, namely, Ig-I, Ig-II, and Ig-III. The Ig-III domain is regulated by alternative splicing, which produces either the IIIb isoforms, FGFR1(IIIb)–FGFR3(IIIb), or the IIIc isoforms, FGFR1(IIIc)–FGFR3(IIIc), which have distinct FGF binding specificities [11]. Mesenchymal cells expressing the IIIc-isoform respond to FGF2, also known as basic FGF, and FGF4. By contrast, epithelial cells generally expressing the IIIb isoform consequently respond to FGF7, also known as keratinocyte growth factor (KGF), and FGF10[12]. In fact, cancer cells with low expression of ESRP1/2 and high expression of ZEB1/2, are associated with aggressive behavior and poor prognosis, and express only the IIIc isoforms. Conversely, cells that express low levels of ZEB1/2 and high levels of ESRP1/2 are associated with favorable prognoses, and exhibit constitutive expression of the IIIb isoforms[6].

In this study, we determined the EMT phenotypes of OSCC cells and found that FGFR2-IIIb was ubiquitously expressed in epithelial-like OSCC cells. Among various OSCC cells, we determined that TSU and HOC313 cells exhibited mesenchymal-like phenotypes with high motility. In addition, we found that TSU and HOC313 cells exhibited high levels of phosphorylated extracellular signal-regulated kinase 1/2 (ERK1/2), and expressed low levels of ESRP1/2 along with high levels of ZEB1/2 levels, resulting in constitutive expression of only FGFR1(IIIc). The FGFR1(IIIc) isoform is apparently activated by soluble factors secreted autonomously by these cells and is needed to sustain high-level expression of ZEB1/2. When we antagonized FGFR1 by either using an inhibitor or specific siRNAs, resulting in the inactivation of ERK1/2 and repression of ZEB1/ZEB2, we observed partial phenotypic changes to epithelial traits. Therefore, sustained high-level expression of ZEB1/2 mediated by the FGFR1c-ERK pathway may maintain the mesenchymal-like phenotypes of OSCC cells.

Materials and methods

Cell culture

Human OSCC, TSU, HOC313, OBC-01, OSC-19, OSC-20, and OTC-04 cells were gifts from Dr. E. Yamamoto and Dr. S. Kawashiri[13]. HSC-2, HSC-3, and HSC-4 were gifts from Dr. F. Momose and Dr. H. Ichijo[14, 15]. Mouse mammary epithelial NMuMG cells, and human OSCC SAS and Ca9-22 cells were also described previously[16]. TSU, HOC313 and HSC-4 cell lines were authenticated by Single Tandem Repeat analysis. All cells were cultured in DMEM (Nacalai Tesque, Kyoto, Japan) supplemented with 4.5 g/L glucose, 10% FBS, 50 U/mL penicillin, and 50 μg/mL streptomycin at 37˚C under a 5% CO_2 atmosphere.

Reagents and antibodies

Recombinant human TGF-β, FGF basic (FGF2), and FGF7 were obtained from R&D Systems (Minneapolis, MN). Rabbit monoclonal anti–phospho-ERK1/2 antibody (#9101S Lot27) was from Cell Signaling (Danvers, MA). Rabbit polyclonal anti-ZEB1 (NBP1-05987 LotA3) and anti-ZEB2 (NBP1-82991 LotB96837) antibodies were obtained from Novus Biologicals (Littleton, CO). Mouse monoclonal anti-Vimentin antibody (M7020 LotM702001111101) was from Dako (Denmark), Mouse monoclonal anti–E-cadherin (610182 Lot5113982) and anti–α-tubulin (T9026) antibodies were from BD Biosciences (Lexington, KY) and Sigma-Aldrich (St. Louis, MO), respectively. SU5402 (#572630) and U0126 (#211–01051) were purchased from Calbiochem (Darmstadt, Germany) and Wako (Osaka, Japan), respectively. AP24534 (S1490) was from Selleck Chemicals (Houston, TX)

Immunoblotting

The procedures used for immunoblotting assays were previously described[17]. Briefly, cells were lysed in lysis buffer (20 mM Tris-HCl [pH7.5], 150 mM NaCl, 1% Nonidet P-40, 5 mM EDTA, 1 mM EGTA, and protease and phosphatase inhibitors). Protein concentration was measured using BCA protein assay reagent (Thermo Fisher Scientific, Waltham, MA). Harvested proteins separated by SDS-PAGE were transferred on to polyvinylidene difluoride membranes. The blots were incubated overnight at 4˚C. Working dilution of primary antibodies was 1:1000. After incubation with secondary HRP-conjugated mouse or rabbit IgG (1:10000, Jackson ImmunoResearch Laboratories) for 1 h, proteins were visualized using Amersham Biosciences ECL Western blotting detection reagent (GE Healthcare). All images were acquired with a Fujifilm LAS-4000 mini imager and analyzed with Image Reader LAS-4000 software (Fujifilm, Tokyo, Japan).

Immunofluorescence labeling

The procedures used for immunofluorescence labeling were previously described[17]. Briefly, cells were fixed in 1:1 acetone-methanol solution and incubated with antibodies diluted with Blocking One solution (1:500, Nacalai Tesque, Kyoto, Japan) for 1 h at room temperature. The cells were then incubated with secondary antibodies and TOPRO (Invitrogen Molecular Probes, Eugene, OR) for 1 h. Fluorescence was examined by using an Olympus FV1000 confocal microscope.

RNA extraction and reverse transcription

Total RNA was extracted using the RNeasy mini kit with DNase treatment (Qiagen, Venlo, Netherlands), and stored at -80˚C until use. Purity of the RNA samples was assessed spectrophotometrically by measuring the $OD_{260/280}$ ratio. The reverse transcription was performed

immediately following the quality control assessment. Two μg of total RNA were then reverse-transcribed into cDNA using the PrimeScript First Strand cDNA synthesis kit (Takara-Bio, Kusatsu, Japan), according to the manufacturer's instructions.

Conventional PCR

Target sequence for conventional PCR primers was 300–500 bp long with a melting temperature of 55–65˚C and a GC content between 45% and 55%. PCR primers were designed using Primer-Blast. Conventional PCR was performed with LA Taq polymerase (TaKaRa). All PCR conditions included an initial denaturation for 2 min at 95˚C. Amplification reactions were performed for 30 cycles under the following conditions: 95˚C for 1 min, 98˚C for 20s, 50˚C for 1 min and 72˚C for 2 min, followed by an extension of 10 min at 72˚C. PCR products were separated on 2% agarose gels, stained with ethidium bromide, and visualized using a Printgraph AE-6932GXES gel detection system (ATTO Corp. Tokyo, Japan). The gene encoding GAPDH was used as an internal control in conventional PCR. The primers used in conventional PCR as follows:

human FGFR1IIIb, forward, 5′-AATGTGACAGAGGCCCAGAG-3′, reverse, 5′-GGAGTCAGCAGACACTGT-3′

human FGFR1IIIc, forward, 5′-ACTGCTGGAGTTAATACCAC-3′ reverse, 5′-GGAGTCAGCAGACACTGT-3′

human FGFR2IIIb, forward, 5′-CACTCGGGGATAAATAGTT-3′, reverse, 5′-ACTCGGAGACCCCTGCCA-3′

human FGFR2IIIc, forward, 5′-CGGTGTTAACACCACGGAC-3′ reverse, 5′-ACTCGGAGACCCCTGCCA-3′

human GAPDH, forward, 5′-CGACCACTTTGTCAAGCTCA-3′, reverse, 5′-CCCTGTTGCT

Quantitative real-time PCR (qPCR)

Target sequence for quantitative real-time PCR (qPCR) was 75–150 bp long with a melting temperature of 55–65˚C and a GC content between 45% and 55%. PCR primers were designed using Primer-Blast. qPCR analyses were performed using Power SYBR Green PCR Master Mix (Applied Biosystems, Foster City, CA) using a Step One Plus thermocycler with fluorescence detection (Applied Biosystems). The relative expression level of each mRNA was normalized against level of *GAPDH* mRNA[18]. The primers used were described previously[6], except the qPCR primers specific for human *FGFR1*, *FGFR2*, and *FGF2*[19, 20].

human *FGFR1*: forward, 5′-TGAGTACGGCAGCATCAACCAC-3′; reverse, 5′-ACTGTTTTGTTGGCGGGCAAC-3′

human *FGFR2*: forward, 5′-TGTGCACAAGCTGACCAAACG-3′; reverse, 5′-AGGCGTGTTGTTATCCTCACCAG-3′

human *FGF2*: forward, 5′-AACCTGCAGACTGCTTTTTGCC; reverse, 5′-ACGTGAGAGCAGAGCATGTGAG

The levels of expressed genes were measured by relative qPCR. A standard curve was always used and ensured by producing a 2-fold dilution series over five points of the most concentrated cDNA sample [20, 21]. For each dilution, qPCR was performed in triplicate for all the PCR primer pairs. The standard curve was constructed by plotting the log of the starting quality of template against the Threshold Cycle (Ct) values obtained. The equation of the linear regression line was used to evaluate whether the qPCR assay was optimized. qPCR detection instruments including 96-well plates were obtained from Applied Biosystems.

To perform reverse transcription-qPCR (RT-qPCR) analyses, cells were seeded in two wells of the tissue culture plate. mRNAs were independently extracted from the cells, and each split into three wells of 96-wells to measure endogenous mRNA levels by RT-qPCR. We repeated these experiments at least two times, and representative results are shown in figures.

RNA interference

Transfection of siRNAs was performed in six-well tissue culture plates using Lipofectamine RNAiMAX transfection reagent (Invitrogen). The final concentration of siRNA was 10 nM. The stealth RNAi siRNA against either human *FGFR1* (#1299001) or mouse *Fgfr1* (#1320001) were purchased from Thermo Fisher Scientific. The sequences of siRNAs against human *FGFR1c* used in this study (Sigma-Aldrich) were as follows;

human *FGFR1c* siRNA #1: GAUGGAGGUGGUUCACUUA

human *FGFR1c* siRNA #2: CGGGUAACUCUAUGGGACU

Cell proliferation assay

Cells were seeded on six-well plates, then trypsinized and counted by hemocytometer. Twenty-four hours after transfection with the siRNAs, cells were seeded in triplicate in 24-well tissue culture plates. Twenty-four hours after seeding, cell count assays were carried out using Cell Count Reagent SF (Nacalai Tesque).

Invasion assay

Boyden chamber migration assays were conducted using transparent PET membrane 24-well 8.0 μm pore size cell culture inserts (BD Falcon, Franklin Lakes, NJ) coated with collagen type I-C (Nitta Gelatin, Osaka, Japan). After cells were seeded in triplicate on the inserts, cells that had not invaded the lower surfaces of the filters were removed from the upper faces of the filters using cotton swabs. Cells that invaded into the lower surfaces of the filters were fixed in acetone:methanol (1:1) and stained with Trypan Blue. Invasion was quantitated by visually counting photographed cells. Cell numbers were evaluated by statistical analysis.

Statistical analyses

Data are presented as means ± SD. Statistical analyses were performed using Student's *t*-test between any two groups.

Results

Evaluation of EMT phenotypes in human OSCC cell lines

To determine the EMT phenotypes of human OSCC cells, we investigated OSCC cell lines by immunoblot and RT-qPCR analyses. Among various OSCC cells, TSU and HOC313 cells expressed high levels of vimentin and low levels of E-cadherin, while other OSCC cells expressed high levels of E-cadherin and low levels of vimentin (Fig 1A, 1B and 1C). HSC-4 cells exhibited a cobblestone-like shape, whereas TSU and HOC313 cells showed a spindle-like shape with great motility compared to other epithelial-like OSCC cells (Fig 1D and 1E), suggesting that both TSU and HOC313 cells show mesenchymal-like trails, whereas other OSCC cells exhibit epithelial-like characteristics.

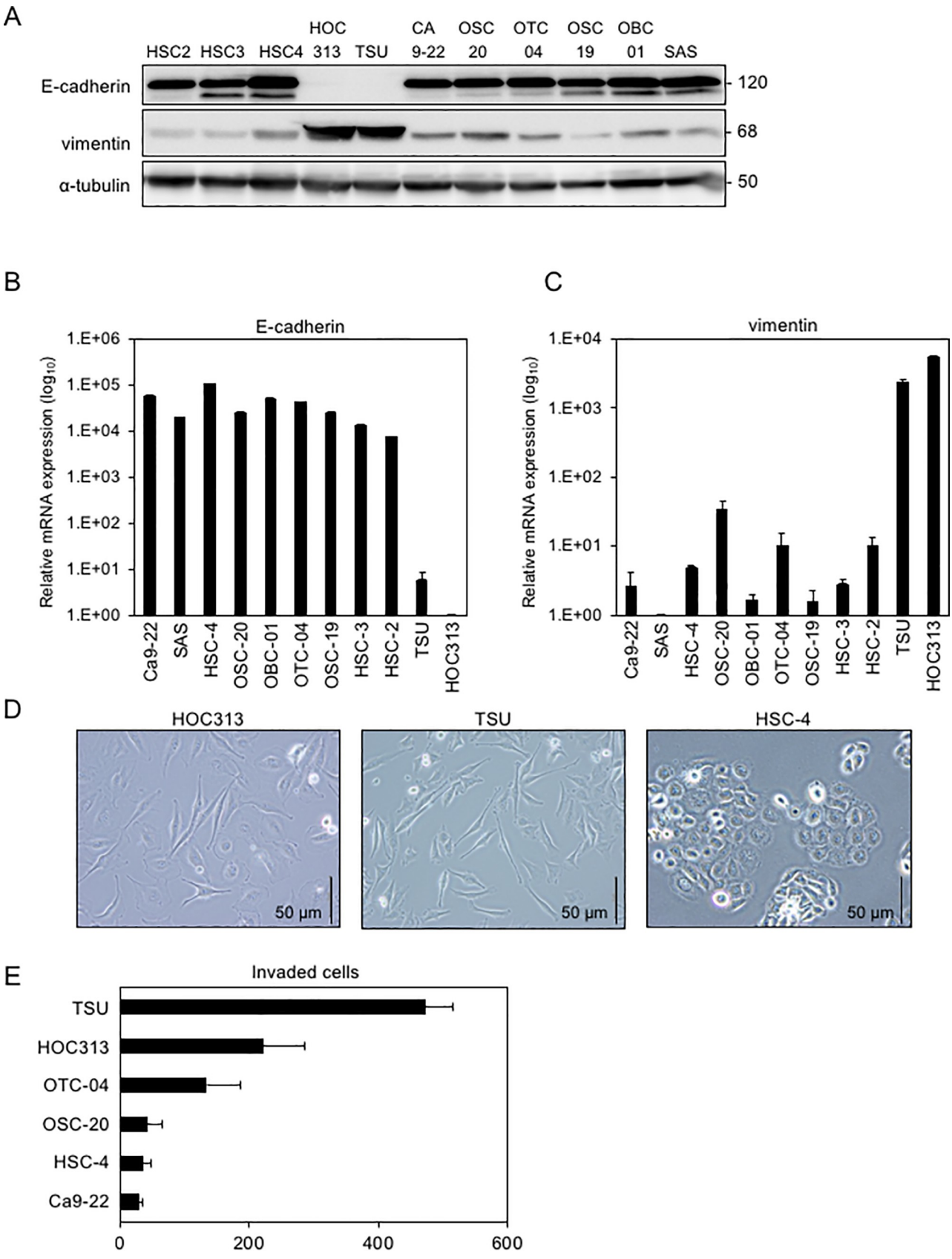
A
HSC2 HSC3 HSC4 HOC 313 TSU CA 9-22 OSC 20 OTC 04 OSC 19 OBC 01 SAS
E-cadherin
vimentin
α-tubulin
120
68
50
B
E-cadherin
Relative mRNA expression (log10)
1.E+06
1.E+05
1.E+04
1.E+03
1.E+02
1.E+01
1.E+00
Ca9-22 SAS HSC-4 OSC-20 OBC-01 OTC-04 OSC-19 HSC-3 HSC-2 TSU HOC313
C
vimentin
Relative mRNA expression (log10)
1.E+04
1.E+03
1.E+02
1.E+01
1.E+00
Ca9-22 SAS HSC-4 OSC-20 OBC-01 OTC-04 OSC-19 HSC-3 HSC-2 TSU HOC313
D
HOC313
TSU
HSC-4
50 μm
50 μm
50 μm
E
Invaded cells
TSU
HOC313
OTC-04
OSC-20
HSC-4
Ca9-22
0
200
400
600

Fig 1. E-cadherin and vimentin expression profiles, and motility of various OSCC cells. (A, B, C) Expression levels of E-cadherin and vimentin were determined by immunoblotting (A) and RT-qPCR (B and C). For immunoblotting, α-tubulin levels were monitored as a loading control (A). The ratio of *E-cadherin* to *GAPDH* mRNAs in HOC313 cells was indicated as "1" (B). The ratio of *vimentin* to *GAPDH* mRNAs in SAS cells was indicated as "1" (C). **(D)** Representative images of showing the morphology of TSU, HOC313, and HSC-4 cells. **(E)** Motility of various OSCC cell lines was determined by transwell assays. Each value represents the mean ± SD of triplicate determinations from a representative experiment. Similar results were obtained from at least three independent experiments (B, C, E).

https://doi.org/10.1371/journal.pone.0217451.g001

Determination of ZEB1/2 expression in OSCC cells

We previously reported that the expression of ZEB1/2 is positively correlated with EMT phenotypes of breast cancer cell lines[6, 7]. In breast cancer, cells with high levels of ZEB1/2 and low levels of ESRP1/2 and E-cadherin are categorized into the "basal-like" subtype of breast cancer with aggressive behavior and poor prognosis[6, 22]. By contrast, cells that express low levels of ZEB1/2 along with high levels of ESRP1/2 and E-cadherin were categorized into the "luminal" subtype of breast cancer with relatively good prognosis[6, 22]. Similar to the basal-like subtype, mesenchymal-like OSCC, TSU and HOC313, cells exhibited high levels of *ZEB1* and *ZEB2* mRNA and low levels of *ESRP1* and *ESRP2* mRNA (Fig 2A and S1 Fig). On the other hand, the other epithelial-like OSCC cells showed the opposite expression profiles for these mRNAs (Fig 2A and S1 Fig). OSCC tissues expressing high levels of *ZEB1* also showed high levels of *ZEB2* (S1 Fig). However, the expression levels of neither Snail, Slug nor Twist were faithfully correlated with the phenotypes of OSCC cells used in this study (S1 Fig).

We also previously reported that ZEB1/2 are preferentially recruited to the promoter region of *ESRP1* where they suppress the transcription of *ESRP1* in breast cancer cells[6]. When both *ZEB1* and *ZEB2* are simultaneously knocked down with their specific siRNAs, *ESRP1* expression was dramatically upregulated in HOC313 cells, whereas *ESRP2* was not (Fig 2B); this phenotype did not occur when either ZEB1 or ZEB2 was knocked down alone. Since ESRP1, rather than ESRP2, causes the alternative splicing-mediated isoform switching between *RAC1b* transcripts in OSCC cells[10], we determined the relative abundance of alternative splicing variants of *FGFR1* and *FGFR2*. Interestingly, all epithelial-like OSCC cells expressed FGFR2(IIIb), which was not detected in either TSU or HOC313 cells. By contrast, TSU and HOC313 cells expressed only FGFR1(IIIc) (Fig 2C). Indeed, analyses using the TCGA dataset indicated a positive correlation between ZEB1/2 and FGFR1, and negative correlation between ZEB1/2 and FGFR2 (S2 Fig). HSC-2 cells expressed both the IIIb and IIIc isoforms of FGFRs (Fig 2C), probably due to low expression of both *ESRP1* and *ESRP2*, whereas OBC-01 cells also expressed both isoforms with moderate expression of *ESRP1/2* (Fig 2A, and S1 Fig). In HSC-4 cells, FGFR2 was localized to the plasma membrane while only negligible amounts of FGFR1 were detected. TSU cells exhibited almost no detectable FGFR2 while the intracellular localization of FGFR1 was diffused (Fig 2D).

Constitutive activation of ERK1/2 in mesenchymal-like OSCC cells

FGF2 and FGF4 bind preferentially to the IIIc-isoform, whereas FGF7 and FGF10 bind exclusively to the IIIb-isoform[11]. In HSC-4 and OTC-04 cells, FGF7 induced the phosphorylation of ERK1/2, but FGF2 did not due to the lack of IIIc-isoform expression in the cells (Fig 3A). Indeed, overexpression of FGFR1(IIIc) in OTC04 and HSC4 cells transduced signals to activate Activator protein (AP)-1 luciferase reporter in response to FGF2 (S3 Fig)[23]. Interestingly, ERK1/2 phosphorylation in mesenchymal-like TSU and HOC313 cells was detected even under serum-free culture conditions (Fig 3B). Although FGF2 induced only slight phosphorylation of ERK1/2 in cells that express FGFR1(IIIc) (Fig 3B), treatment with the FGFR1 inhibitor, SU5402, almost completely inhibited phosphorylation of ERK1/2, suggesting the

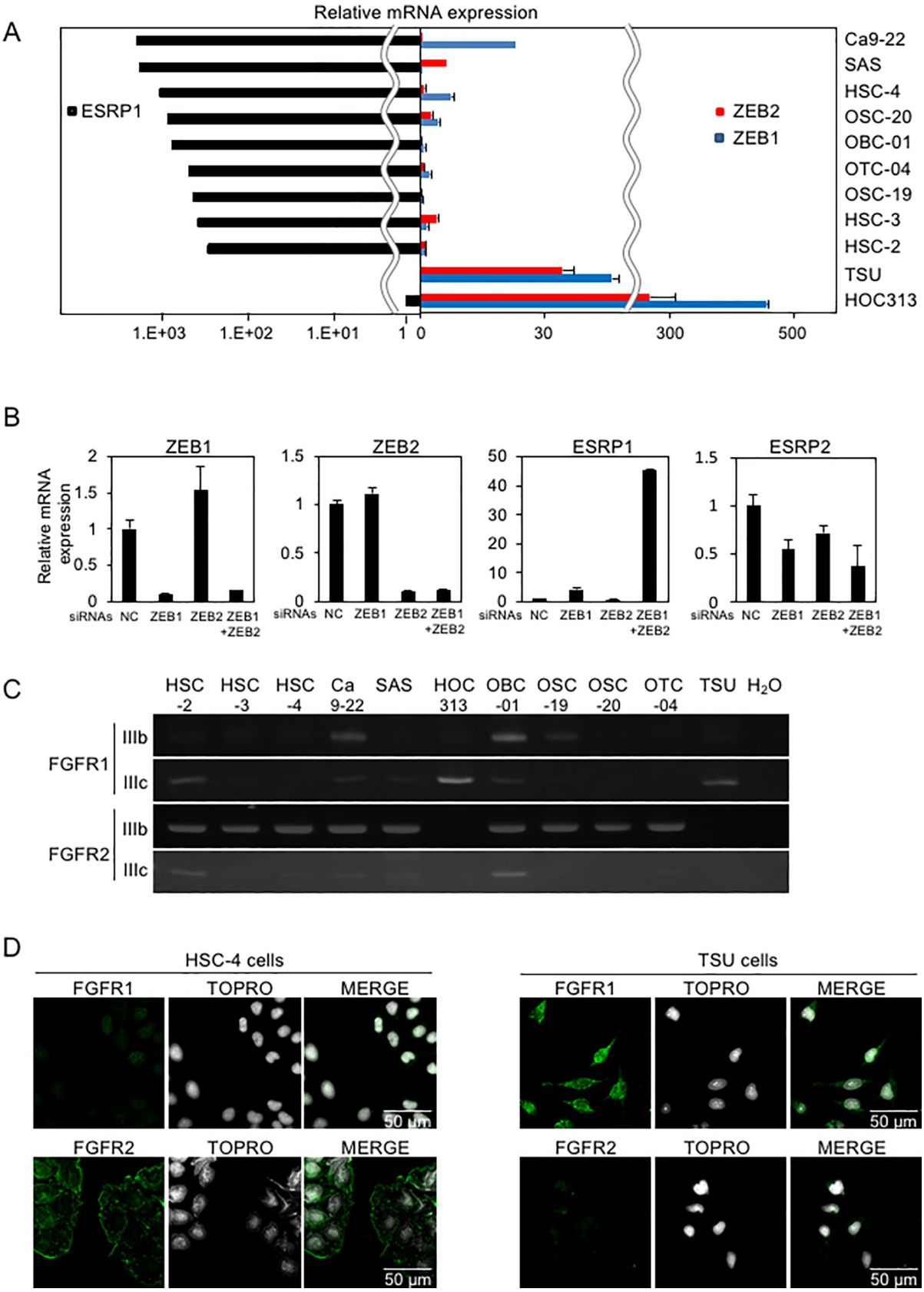
A
Relative mRNA expression
ESRP1
ZEB2
ZEB1
Ca9-22
SAS
HSC-4
OSC-20
OBC-01
OTC-04
OSC-19
HSC-3
HSC-2
TSU
HOC313
1.E+03
1.E+02
1.E+01
1
0
30
300
500
B
ZEB1
ZEB2
ESRP1
ESRP2
Relative mRNA expression
siRNAs NC ZEB1 ZEB2 ZEB1 +ZEB2
C
HSC -2
HSC -3
HSC -4
Ca 9-22
SAS
HOC 313
OBC -01
OSC -19
OSC -20
OTC -04
TSU
H2O
FGFR1
IIIb
IIIc
FGFR2
IIIb
IIIc
D
HSC-4 cells
TSU cells
FGFR1
TOPRO
MERGE
FGFR2
TOPRO
MERGE
50 μm

Fig 2. *ESRP1*, *ZEB1*, and *ZEB2* expression profiles in OSCC cells. (A) mRNA levels of the expression of *ESRP1*, *ZEB1*, and *ZEB2* were determined by RT-qPCR. Each value was normalized to the level of *GAPDH* mRNA in the same sample. The ratio of *ESRP1* to *GAPDH* mRNAs in HOC313 cells was indicated as "1". The expression of ESRP1 mRNA was negligibly detected in TSU cells (left panel). The ratio of *ZEB1/2* to *GAPDH* mRNAs in the lowest expression cells was indicated as "1". **(B)** TSU cells were transfected with siRNAs against *ZEB1*, *ZEB2*, or both, and *ESRPs* mRNA level was determined by RT-qPCR. NC, non-specific control siRNA. Each value represents the mean ± SD of triplicate determinations from a representative experiment. Similar results were obtained in at least three independent experiments. **(C)** The expression of FGFR isoforms in OSCC cells was determined by conventional RT-PCR. **(D)** Subcellular localization of endogenous FGFR1 and FGFR2 proteins was determined by anti–FGFR1 and–FGFR2 antibodies, respectively, in HSC-4 and TSU cells.

https://doi.org/10.1371/journal.pone.0217451.g002

involvement of autocrine factors that activate FGFR1(IIIc). To test this possibility, conditioned medium from TSU cells was added to mouse mammary epithelial NMuMG cells pretreated with TGF-β to express Fgfr1(IIIc)[17]. The conditioned medium from TSU cells, but not HSC-4 cells, caused a slight increase in ERK1/2 phosphorylation, while either pretreatment with SU5402 or transfection with mouse *Fgfr1* siRNA into TGF-β-treated NMuMG cells repressed it (Fig 3C and S3 Fig).

Indeed, *FGF2* mRNA was highly expressed in mesenchymal-like TSU and HOC313 cells (Fig 3D). SU5402 inhibited phosphorylation of ERK1/2 in a dose-dependent manner in HOC313 and TSU cells (Fig 3E). In addition, the representative epithelial marker, E-cadherin, was upregulated by SU5402, whereas the representative mesenchymal markers, N-cadherin and vimentin, as well as ZEB1/2 were suppressed at both the mRNA and protein levels (Fig 3F and 3G). These findings suggest that mesenchymal-like OSCC cells autonomously secrete factors, including FGF2, to activate FGFR(IIIc), and that blocking FGFR1 signaling regulates the expression of EMT markers. Importantly, ZEB1 was retained at high levels in mesenchymal-like TSU and HOC313 cells, which was repressed by FGFR1 inhibitor. When ERK1/2 was also inactivated by the MEK inhibitor, U0126, ZEB1 was downregulated (Fig 3H), strongly suggesting that high-level expression of ZEB1 is sustained by constitutive activation of ERK1/2 mediated by FGFR(IIIc), which is activated by soluble factors secreted autonomously by the cells.

Effects of *FGFR1* siRNAs in mesenchymal-like TSU cells

In addition to SU5402, to elucidate the functions of FGFR1 in mesenchymal-like TSU cells, we used siRNAs against human *FGFR1*. Three kinds of *FGFR1*-targeted siRNAs effectively knocked down endogenous *FGFR1*, as determined by conventional RT-PCR analyses (Fig 4A). ERK1/2 phosphorylation and ZEB1 expression in TSU cells were reduced by *FGFR1* siRNAs (Fig 4B and 4C). The repressive effects of *FGFR1* siRNAs on ZEB1 levels were also observed in the basal-like breast cancer, Hs-578T, and MDA-MB231 cells, which expressed FGFR1(IIIc) isoform (S3 Fig)[6]. In addition, cell morphology was slightly altered from a spindle shape to a cobblestone-like shape (Fig 4D). Immunofluorescence analyses indicated that E-cadherin was upregulated and localized to the plasma membrane in some TSU cells (Fig 4E).

Invasion properties were inhibited by SU5402, which was accompanied with the reduced cell number (Fig 4F and 4G). Another FGFR1 inhibitor, AP24534, also suppressed the motility of TSU cells with affecting ERK1/2 phosphorylation and ZEB1 expression (S3 Fig). In addition, siRNAs against *FGFR1* inhibited motile properties in TSU and HOC313 cells (Fig 4H and 4I). Based on previous report[24], we generated siRNAs against human *FGFR1c*. Similar to *FGFR1* siRNAs, *FGFR1c* siRNAs also suppressed motile properties in both cells (Fig 4J and 4K). Taken together, FGFR(IIIc) isoforms, which are predominantly expressed in mesenchymal-like OSCC cells, would be constitutively activated by factors secreted autonomously by the cells and sustain ZEB1 expression at high levels through the activating ERK1/2 pathway, leading to maintaining EMT phenotypes.

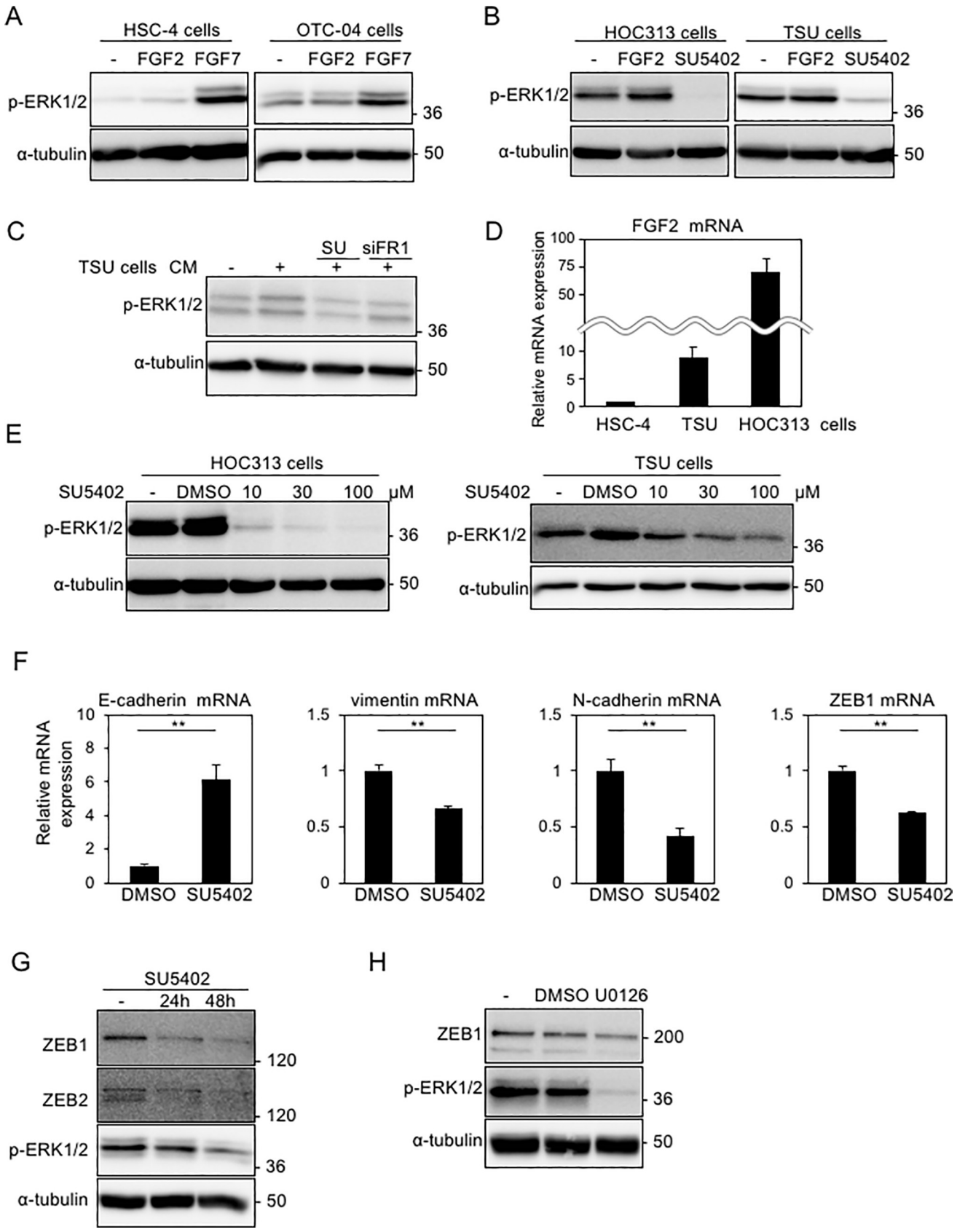
A
HSC-4 cells
OTC-04 cells
- FGF2 FGF7
- FGF2 FGF7
p-ERK1/2
α-tubulin
36
50
B
HOC313 cells
TSU cells
- FGF2 SU5402
- FGF2 SU5402
p-ERK1/2
α-tubulin
36
50
C
TSU cells CM
SU
siFR1
- + + +
p-ERK1/2
α-tubulin
36
50
D
FGF2 mRNA
Relative mRNA expression
100
75
50
10
5
0
HSC-4
TSU
HOC313 cells
E
HOC313 cells
SU5402 - DMSO 10 30 100 μM
p-ERK1/2
α-tubulin
36
50
TSU cells
SU5402 - DMSO 10 30 100 μM
p-ERK1/2
α-tubulin
36
50
F
E-cadherin mRNA
vimentin mRNA
N-cadherin mRNA
ZEB1 mRNA
Relative mRNA expression
**
10
8
6
4
2
0
1.5
1
0.5
0
DMSO SU5402
G
SU5402
- 24h 48h
ZEB1
ZEB2
p-ERK1/2
α-tubulin
120
120
36
50
H
- DMSO U0126
ZEB1
p-ERK1/2
α-tubulin
200
36
50

Fig 3. SU5402, FGFR1 inhibitor, affects the EMT transcription factors. (A, B) ERK1/2 phosphorylation (p-ERK1/2) was determined by immunoblotting in HSC-4 and OTC-04 treated for 30 min with 30 ng/ml FGF2 or 30 ng/ml FGF7 in the presence of 10% FBS (A) and in TSU and HOC313 cells treated for 1 h with 30 ng/ml FGF2 or 30 μM SU5402 in the absence of FBS (B). F2, FGF2; F7, FGF7; SU, SU5402. **(C)** We have previously reported that, after treatment with TGF-β, NMuMG cells underwent EMT with the IIIc-isoform of FGFR1[17]. After NMuMG cells pretreated with TGF-β were transfected with mouse *Fgfr1* siRNA or treated with SU5402, the cells were further incubated in culture medium (CM) from TSU cells. SU, SU5402; siFR1, siRNA against mouse *Fgfr1*. **(D)** *FGF2* mRNA levels were determined by RT-qPCR analyses. The ratio of *FGF2* mRNA to *GAPDH* mRNA in HSC-4 cells was indicated as "1". Each value represents the mean ± SD of triplicate determinations from a representative experiment. Similar results were obtained in at least three independent experiments. **(E)** ERK1/2 phosphorylation (p-ERK1/2) in TSU and HOC313 cells were monitored in the presence of the indicated concentration of SU5402 for 1 h under serum-free culture conditions, followed by immunoblot analysis. **(F, G)** Expression of the indicated genes in TSU cells under serum-free culture conditions was determined by RT-qPCR (F) and immunoblot (G) analyses, following treatment with 10 μM SU5402. Each value represents the mean ± SD of triplicate determinations from a representative experiment. Similar results were obtained from at least three independent experiments. p values were determined by Student's t-test. $^{**}p < 0.01$. **(H)** TSU cells treated with 10 μM U0126 in the absence of FBS were subjected to immunoblotting with the indicated antibodies. α-tubulin was used as a loading control (A, B, C, E, G, and H).

https://doi.org/10.1371/journal.pone.0217451.g003

Discussion

In the study we found that, similar to the basal-like subtype of breast cancer, OSCC cells with high levels of ZEB1/2 and low levels of E-cadherin and ESRP1/2 exhibited mesenchymal-like traits with FGFR(IIIc) isoforms. By contrast, OSCC cells with low levels of ZEB1/2, and high levels of E-cadherin and ESRP1/2 exhibited epithelial-like traits with FGFR(IIIb) isoforms, similar to the luminal-like subtype of breast cancer[6]. Importantly, mesenchymal-like cancer cells expressed FGFR1(IIIc), whereas epithelial-like cancer cells expressed FGFR2(IIIb) (Fig 2). During TGF-β–induced EMT in NMuMG cells, TGF-β induces ZEB1/2 expression while repressing ESRP1/2 expression, leading to isoform switching from FGFR2(IIIb) to FGFR1 (IIIc), but not to FGFR2(IIIc)[6, 17]. When ESRP1 was ectopically overexpressed during TGF-β–induced EMT, FGFR2(IIIb) changed to FGFR1(IIIb)[6]. Taken together, conversion of FGFR2(IIIb) to FGFR1(IIIc) during EMT requires transcriptional regulation and alternative splicing machinery dependent on ESRP1/2. These observations prompted us to investigate the potential involvement of TGF-β that is secreted autonomously by OSCC cells. When endogenous TGF-β was inhibited by a TGF-β receptor inhibitor, FGFR isoform switching and the regulation of *FGFR1* and *FGFR2* mRNA were not significantly altered in OSCC cells, in agreement with our previous observation in breast cancer cells[6]. Conversely, TGF-β treatment also failed to regulate both isoform switching and transcription of FGFR1/2. Therefore, in addition to isoform switching by ESRP1/2-mediated alternative splicing, signaling pathway(s) apart from the TGF-β pathway may be involved in the expression of FGFR1(IIIc) in mesenchymal-like OSCC.

ZEB1 and ZEB2 are known to be extensively upregulated by TGF-β in both normal epithelial cells and cancer cells[25]. ZEB1/2 suppress the expression of ESRP1 by binding to its promoter region, thereby inducing the expression of FGFR(IIIc) isoforms[6] whereas antagonizing FGFR1(IIIc) downregulates ZEB1 expression (Fig 3). These findings suggest that, during the early stages of cancer, TGF-β accumulates gradually in cancerous tissues[26, 27] where it subsequently induces EMT by inducing ZEB1/2 expression. Once ZEB1/2 expression has been upregulated, the cells will express FGFR(IIIc) isoforms. Soluble factors, such as FGF2, secreted autonomously by cancer cells undergoing EMT, activate FGFR(IIIc) and ERK pathways to sustain high ZEB1/2 levels. Because FGF2 is itself known to be induced by either TGF-β or FGF2[28, 29], a positive feedback loop of autocrine FGF2 signaling can be initiated by TGF-β and sustained by FGF2, thereby maintaining mesenchymal phenotypes. If this positive feedback loop was generated, the cells maintain EMT phenotypes even in the absence of TGF-β. Following that, abundant distribution of FGF2/4 in the cancer microenvironment further stimulates FGFR(IIIc) isoforms in cancer cells undergoing EMT and sustains EMT phenotypes even in the vascular and lymphatic systems. Thus, the addiction of mesenchymal phenotypes of OSCC cells could be switched from the TGF-β axis to the FGF–FGFR axis. Finally, ZEB1

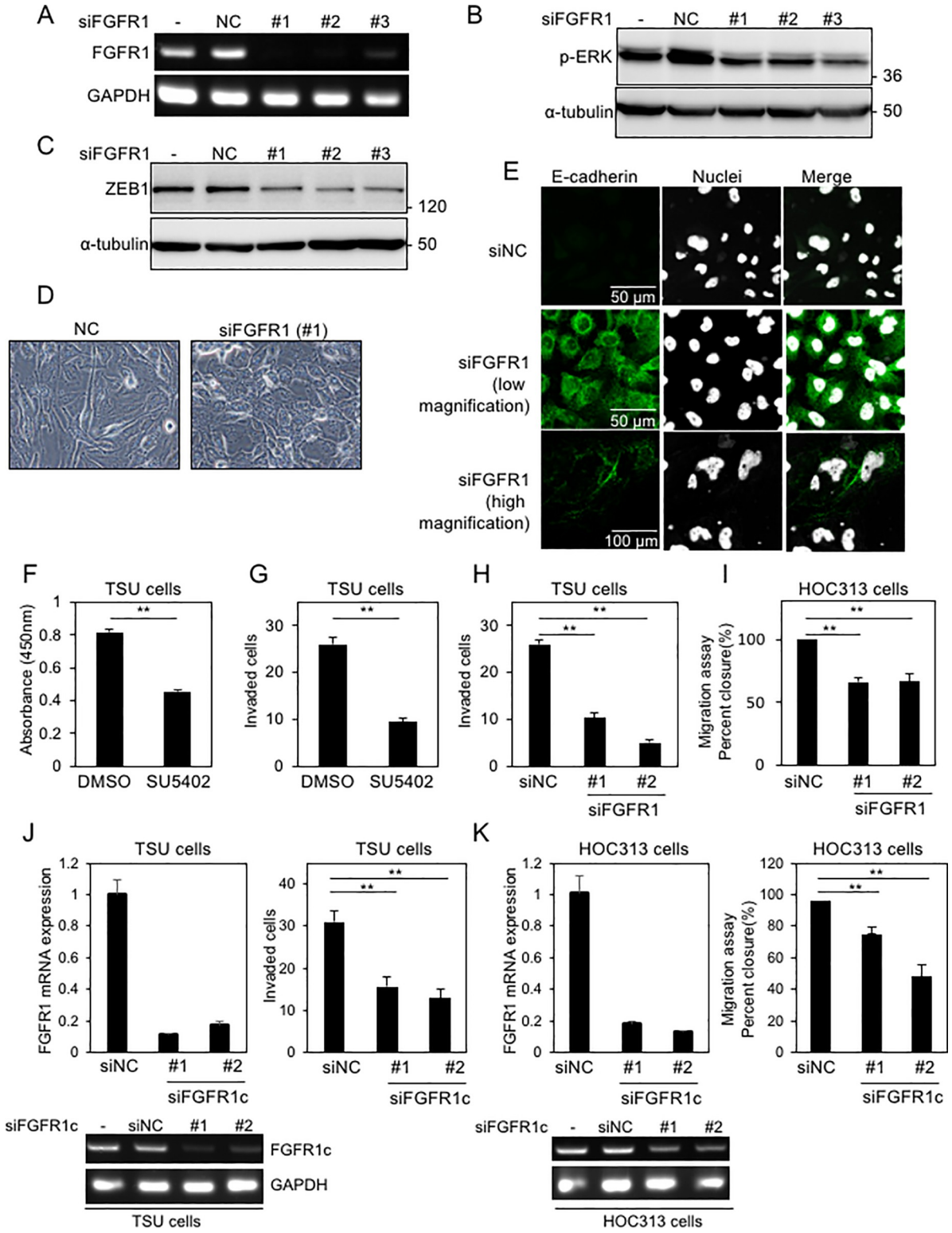

Fig 4. *FGFR1* siRNAs attenuate the malignant phenotypes of cancer cells. (A) mRNA from TSU cells transfected with siRNAs against *FGFR1* (si*FGFR1*) were subjected to conventional RT-PCR to determine the levels of endogenous *FGFR1*. **(B, C, D)** After transfection with si*FGFR1* in TSU cells, phosphorylation of ERK1/2 (p-ERK1/2) (B), ZEB1 levels (C), and cell morphology (D) were determined. **(E)** TSU cells transfected with si*FGFR1* were subjected to immunofluorescence analyses. Low magnification, 40×; high magnification, 80×. **(F, G, H, I)** After either treatment with SU5402 or transfection with si*FGFR1* in TSU and HOC313 cells, the number of cells and invasive properties

were determined under serum-free culture conditions. **(J and K)** After transfection with si*FGFR1c* in TSU and HOC313 cells, invasive and migratory properties were determined under serum-free culture conditions in TSU and HOC313 cells, respectively. siNC, non-specific control siRNA. Each value represents the mean ± SD of triplicate determinations from a representative experiment. Similar results were obtained from at least three independent experiments. p values were determined by Student's t-test. $^{*}p < 0.01$.

https://doi.org/10.1371/journal.pone.0217451.g004

and ZEB2 promote the recruitment of DNA methyltransferase to the promoter region by interacting with each other, resulting in epigenetic regulation of EMT marker genes such as E-cadherin[7].

FGF2 was previously reported to be produced by the cells of primary prostate carcinomas with metastasis, and that FGF2 causes the switching of FGFR isoforms from IIIb to IIIc[30]. Similar to these observations based on prostate cancer, mesenchymal-like OSCC cells also produced soluble factors that activate FGFR1(IIIc) (Fig 3B and 3C). However, the pathological significance of isoform switching from FGFR2(IIIb) to FGFR1(IIIc) isoform remains unclear, because both FGFR isoforms have almost the same intracellular structure and tyrosine kinase domains. N-cadherin has been reported to interact selectively with FGFR1(IIIc)[31], suggesting that N-cadherin, expressed in mesenchymal-like OSCC cells, can cooperate to transduce unique signals to sustain high-level expression of ZEB1/2.

An antibody that preferentially recognizes only FGFR1(IIIc) was recently developed[32]. However, antibodies that preferentially recognize specific isoforms of other FGFRs have yet to be generated, probably due to the high degree of structural similarity between their extracellular domains. Therefore, diagnosis and therapy, which specifically target the IIIc isoforms, will require the development of methods that can recognize the IIIc isoform proteins specifically, as well as anti-tumor drugs that can target the IIIc isoform proteins specifically.

Supporting information

S1 File.
(DOC)

S1 Fig. mRNA levels of ESRP and EMT-TFs in OSCC cells. (A) *ESRP2* mRNA level was determined by RT-qPCR in OSCC cells. Each value was normalized to the level of *GAPDH* mRNA in the same sample. The ratio of *ESRP2* to *GAPDH* mRNAs in HOC313 cells was indicated as "1". **(B)** Correlations between *ZEB1* and *ZEB2* mRNAs in oral cancer tissues from oral SCC patients in The Cancer Genome Atlas (TCGA) dataset were shown. TCGA is available from the website of The Cancer Genome Atlas program (National Cancer Institute). *ZEB1* and *ZEB2* mRNA expression in oral squamous cell carcinoma (SCC) patients were extracted from TCGA's data portal (GSE37991). Statistical analysis revealed a positive correlation between the expression levels of *ZEB1* and *ZEB2* mRNA in 40 patients of oral SCC. **(C)** Expression level of Snail (*SNAI1*), Slug (*SNAI2*) and *Twist* mRNA was determined by RT-qPCR in OSCC cells. Each value was normalized to the level of *GAPDH* mRNA in the same sample. The ratio of *Snail* to *GAPDH* mRNAs and *Slug* to *GAPDH* mRNAs in HSC-2 cells was indicated as "1". The ratio of *Twist* to *GAPDH* mRNAs in OSC-19 cells was indicated as "1". Data are presented as means ± SD.
(TIFF)

S2 Fig. Correlations between ZEB1/ZEB2 and FGFR1/FGFR2 in oral cancer tissues. (A, B) Correlations between ZEB1/ZEB2 and FGFR1/FGFR2 in oral cancer tissues from oral SCC patients in TCGA dataset were shown. TCGA is available from the website of The Cancer Genome Atlas program (National Cancer Institute). *ZEB1*, *ZEB2*, *FGFR1*, and *FGFR2* mRNA expression in oral squamous cell carcinoma (SCC) patients were extracted from TCGA's data

portal (GSE37991). Statistical analysis revealed a positive correlation between the expression levels of *FGFR1* and *ZEB1* (left) or *ZEB2* (right) mRNA (A), and a negative correlation between the expression levels of *FGFR2* and *ZEB1* (left) or *ZEB2* (right) mRNA (B) in 40 patients of oral SCC.
(TIFF)

S3 Fig. Roles of FGFR1c in cancer cells. (A) OTC-04 and HSC4 cells were cotransfected with AP-1 promoter-reporter construct (Ap-1 Luc.) in combination with FGFR1c-expression plasmids. At 24 h after transfection, the cells were stimulated with either FGF-7 or FGF-2. Twelve h later, the cells were harvested and assayed for luciferase activity. **(B)** After NMuMG cells were pretreated with TGF-β, the cells were further incubated in the conditioned medium (CM) from either HSC4 or TSU cells. FGF2 was used as a positive control. **(C)** The basal-like subtype of breast cancer cells, Hs-578T and MDA-MB231 cells, are known to express FGFR1 (IIIc) [6]. ZEB1 levels were also determined in these cells transfected with si*FGFR1*. **(D)** TSU cells treated with 10 μM AP24534 in the absence of FBS were subjected to immunoblotting using the indicated antibodies (top panels) and to Boyden chamber assays (bottom panel). α-tubulin was used as a loading control (B, C and D). Each value represents the mean ± SD of triplicate determinations from a representative experiment. Similar results were obtained from at least three independent experiments. p values were determined by Student's t-test.
$^{**}p < 0.01$.
(TIFF)

Acknowledgments

We would like to thank Dr. T. Shirakihara and Dr. N. D. Sinh for their helpful advice.

Author Contributions

Conceptualization: Masao Saitoh.

Data curation: Ryosuke Nakamura, Masao Saitoh.

Formal analysis: Asami Hotta Osada, Masao Saitoh.

Funding acquisition: Masao Saitoh.

Investigation: Asami Hotta Osada, Kaori Endo, Yujiro Kimura, Kei Sakamoto, Ryosuke Nakamura, Kaname Sakamoto, Masao Saitoh.

Methodology: Masao Saitoh.

Project administration: Masao Saitoh.

Resources: Masao Saitoh.

Supervision: Koichiro Ueki, Kunio Yoshizawa, Keiji Miyazawa, Masao Saitoh.

Validation: Masao Saitoh.

Writing – original draft: Masao Saitoh.

Writing – review & editing: Keiji Miyazawa.

References

1. Argiris A, Karamouzis MV, Raben D, Ferris RL. Head and neck cancer. Lancet. 2008; 371(9625):1695–1709. https://doi.org/10.1016/S0140-6736(08)60728-X PMID: 18486742.

2. Noguti J, De Moura CF, De Jesus GP, Da Silva VH, Hossaka TA, Oshima CT, et al. Metastasis from oral cancer: an overview. Cancer Genomics Proteomics. 2012; 9(5):329–35. PMID: 22990112.
3. Nieto MA. Context-specific roles of EMT programmes in cancer cell dissemination. Nat. Cell Biol. 2017; 19(5):416–418. https://doi.org/10.1038/ncb3520 PMID: 28446813.
4. Saitoh M. Involvement of partial EMT in cancer progression. J. Biochem. 2018; 164(4):257–64. https://doi.org/10.1093/jb/mvy047 PMID: 29726955.
5. Shibue T, Weinberg RA. EMT, CSCs, and drug resistance: the mechanistic link and clinical implications. Nat. Rev. Clin. Oncol. 2017; 14(10):611–629. https://doi.org/10.1038/nrclinonc.2017.44 PMID: 28397828; PubMed Central PMCID: PMC5720366.
6. Horiguchi K, Sakamoto K, Koinuma D, Semba K, Inoue A, Inoue S, et al. TGF-β drives epithelial-mesenchymal transition throughδEF1-mediated downregulation of ESRP. Oncogene. 2012; 31(26):3190–3201. Epub 2011/11/01. https://doi.org/10.1038/onc.2011.493 PMID: 22037216; PubMed Central PMCID: PMC3391666.
7. Fukagawa A, Ishii H, Miyazawa K, Saitoh M. δEF1 associates with DNMT1 and maintains DNA methylation of the E-cadherin promoter in breast cancer cells. Cancer Med. 2015; 4(1):125–135. Epub 2014/10/16. https://doi.org/10.1002/cam4.347 PMID: 25315069; PubMed Central PMCID: PMC4312126.
8. Warzecha CC, Sato TK, Nabet B, Hogenesch JB, Carstens RP. ESRP1 and ESRP2 are epithelial cell-type-specific regulators of FGFR2 splicing. Mol. Cell. 2009; 33(5):591–601. https://doi.org/10.1016/j.molcel.2009.01.025 PMID: 19285943; PubMed Central PMCID: PMC2702247.
9. Warzecha CC, Jiang P, Amirikian K, Dittmar KA, Lu H, Shen S, et al. An ESRP-regulated splicing programme is abrogated during the epithelial-mesenchymal transition. EMBO J. 2010; 29(19):3286–3300. Epub 2010/08/17. https://doi.org/10.1038/emboj.2010.195 PMID: 20711167; PubMed Central PMCID: PMC2957203.
10. Ishii H, Saitoh M, Sakamoto K, Kondo T, Katoh R, Tanaka S, et al. Epithelial Splicing Regulatory Proteins 1 (ESRP1) and 2 (ESRP2) Suppress Cancer Cell Motility via Different Mechanisms. J. Biol. Chem. 2014; 289(40):27386–27399. Epub 2014/08/22. https://doi.org/10.1074/jbc.M114.589432 PMID: 25143390; PubMed Central PMCID: PMC4183779.
11. Eswarakumar VP, Lax I, Schlessinger J. Cellular signaling by fibroblast growth factor receptors. Cytokine Growth Factor Rev. 2005; 16(2):139–149. https://doi.org/10.1016/j.cytogfr.2005.01.001 PMID: 15863030.
12. Holzmann K, Grunt T, Heinzle C, Sampl S, Steinhoff H, Reichmann N, et al. Alternative Splicing of Fibroblast Growth Factor Receptor IgIII Loops in Cancer. J. Nucleic. Acids. 2012; 2012:950508. https://doi.org/10.1155/2012/950508 PMID: 22203889; PubMed Central PMCID: PMC3238399.
13. Yoshizawa K, Nozaki S, Okamune A, Kitahara H, Ohara T, Kato K, et al. Loss of maspin is a negative prognostic factor for invasion and metastasis in oral squamous cell carcinoma. J. Oral Pathol. Med. 2009; 38(6):535–539. https://doi.org/10.1111/j.1600-0714.2009.00762.x PMID: 19473451.
14. Momose F, Araida T, Negishi A, Ichijo H, Shioda S, Sasaki S. Variant sublines with different metastatic potentials selected in nude mice from human oral squamous cell carcinomas. J. Oral Pathol. Med. 1989; 18(7):391–395. https://doi.org/10.1111/j.1600-0714.1989.tb01570.x PMID: 2585303.
15. Ichijo H, Momose F, Miyazono K. Biological effects and binding properties of transforming growth factor-β on human oral squamous cell carcinoma cells. Exp. Cell Res. 1990; 187(2):263–269. https://doi.org/10.1016/0014-4827(90)90090-w PMID: 2156718.
16. Nakamura R, Ishii H, Endo K, Hotta A, Fujii E, Miyazawa K, et al. Reciprocal expression of Slug and Snail in human oral cancer cells. PloS one. 2018; 13(7):e0199442. https://doi.org/10.1371/journal.pone.0199442 PMID: 29969465; PubMed Central PMCID: PMC6029773.
17. Shirakihara T, Horiguchi T, Miyazawa M, Ehata S, Shibata T, Morita I, et al. TGF-β regulates isoform switching of FGF receptors and epithelial-mesenchymal transition. EMBO J. 2011; 30(4):783–795. https://doi.org/10.1038/emboj.2010.351 PMID: 21224849
18. Pfaffl MW, Tichopad A, Prgomet C, Neuvians TP. Determination of stable housekeeping genes, differentially regulated target genes and sample integrity: BestKeeper—Excel-based tool using pair-wise correlations. Biotechnol. Lett. 2004; 26(6):509–515. PMID: 15127793.
19. Johnson G, Nolan T, Bustin SA. Real-time quantitative PCR, pathogen detection and MIQE. Methods Mol. Biol. 2013; 943:1–16. https://doi.org/10.1007/978-1-60327-353-4_1 PMID: 23104279.
20. Bustin SA, Benes V, Garson JA, Hellemans J, Huggett J, Kubista M, et al. The MIQE guidelines: minimum information for publication of quantitative real-time PCR experiments. Clin. Chem. 2009; 55(4):611–622. https://doi.org/10.1373/clinchem.2008.112797 PMID: 19246619.
21. Taylor S, Wakem M, Dijkman G, Alsarraj M, Nguyen M. A practical approach to RT-qPCR-Publishing data that conform to the MIQE guidelines. Methods. 2010; 50(4):S1–5. https://doi.org/10.1016/j.ymeth.2010.01.005 PMID: 20215014.

22. Neve RM, Chin K, Fridlyand J, Yeh J, Baehner FL, Fevr T, et al. A collection of breast cancer cell lines for the study of functionally distinct cancer subtypes. Cancer Cell. 2006; 10(6):515–527. Epub 2006/12/13. S1535-6108(06)00314-X [pii] https://doi.org/10.1016/j.ccr.2006.10.008 PMID: 17157791; PubMed Central PMCID: PMC2730521.

23. Jibiki I, Hashimoto S, Maruoka S, Gon Y, Matsuzawa A, Nishitoh H, et al. Apoptosis signal-regulating kinase 1-mediated signaling pathway regulates nitric oxide-induced activator protein-1 activation in human bronchial epithelial cells. Am. J. Respir. Crit. Care Med. 2003; 167(6):856–861. https://doi.org/10.1164/rccm.2204042 PMID: 12623859.

24. Sonvilla G, Allerstorfer S, Heinzle C, Stattner S, Karner J, Klimpfinger M, et al. Fibroblast growth factor receptor 3-IIIc mediates colorectal cancer growth and migration. Br. J. Cancer. 2010; 102(7):1145–56. https://doi.org/10.1038/sj.bjc.6605596 PMID: 20234367; PubMed Central PMCID: PMC2853090.

25. Saitoh M. Epithelial-mesenchymal transition is regulated at post-transcriptional levels by transforming growth factor-β signaling during tumor progression. Cancer Sci. 2015; 106(5):481–488. Epub 2015/02/11. https://doi.org/10.1111/cas.12630 PMID: 25664423.

26. Bedossa P, Peltier E, Terris B, Franco D, Poynard T. Transforming growth factor-β1 (TGF-β1) and TGF-β1 receptors in normal, cirrhotic, and neoplastic human livers. Hepatology. 1995; 21(3):760–766. PMID: 7875675.

27. Bierie B, Moses HL. TGF-β and cancer. Cytokine Growth Factor Rev. 2006; 17(1–2):29–40. https://doi.org/10.1016/j.cytogfr.2005.09.006 PMID: 16289860.

28. Matsuyama S, Iwadate M, Kondo M, Saitoh M, Hanyu A, Shimizu K, et al. SB-431542 and Gleevec inhibit transforming growth factor-β-induced proliferation of human osteosarcoma cells. Cancer Res. 2003; 63(22):7791–7798. PMID: 14633705.

29. Vlotides G, Chen YH, Eigler T, Ren SG, Melmed S. Fibroblast growth factor-2 autofeedback regulation in pituitary folliculostellate TtT/GF cells. Endocrinology. 2009; 150(7):3252–3258. https://doi.org/10.1210/en.2008-1625 PMID: 19359387; PubMed Central PMCID: PMC2703553.

30. Nakamoto T, Chang CS, Li AK, Chodak GW. Basic fibroblast growth factor in human prostate cancer cells. Cancer Res. 1992; 52(3):571–577. PMID: 1732045.

31. Suyama K, Shapiro I, Guttman M, Hazan RB. A signaling pathway leading to metastasis is controlled by N-cadherin and the FGF receptor. Cancer Cell. 2002; 2(4):301–314. PMID: 12398894.

32. Buss N, Lapointe JM, de Haan L, Price S, Ahnmark A, Irving L, et al. Monoclonal antibody targeting of fibroblast growth factor receptor 1c causes cardiac valvulopathy in rats. Toxicol. Appl. Pharmacol. 2018; 355:147–155. https://doi.org/10.1016/j.taap.2018.06.033 PMID: 30008375.